Science Advances
AAAS

advances.sciencemag.org/cgi/content/full/4/11/eaau6972/DC1

Supplementary Materials for

Flexible elastomer patch with vertical silicon nanoneedles for intracellular and intratissue nanoinjection of biomolecules

Hyungjun Kim, Hanmin Jang, Bongjoong Kim, Min Ku Kim, Dae Seung Wie, Heung Soo Lee, Dong Rip Kim*, Chi Hwan Lee*

*Corresponding author. Email: dongrip@hanyang.ac.kr (D.R.K.); lee2270@purdue.edu (C.H.L.)

Published 9 November 2018, *Sci. Adv.* **4**, eaau6972 (2018)
DOI: 10.1126/sciadv.aau6972

The PDF file includes:

Other Supplementary Material for this manuscript includes the following:

(available at advances.sciencemag.org/cgi/content/full/4/11/eaau6972/DC1)

Movie S1 (.avi format). An experimental demonstration (scale bar, 2.5 mm; 20× speed) showing the expansion of PDMS when soaked in hexane.
Movie S2 (.avi format). FEA results of displacement for a simplified structure that includes an array (3 cm × 3 cm) of Si NNs on a thin layer of PDMS under the expansion up to 230% in volume.
Movie S3 (.avi format). Continuously recorded live DIC image (scale bar, 15 μm; 4000× speed) of MCF7 cells for 36 hours.
Movie S4 (.avi format). A continuously recorded movie (scale bar, 2 cm; 1× speed) showing a mouse awake with the attached Si NN-patch on the skin.
Movie S5 (.avi format). A continuously recorded movie (scale bar, 2 cm; 1× speed) showing a mouse awake with the implanted Si NN-patch on the subcutaneous muscle.

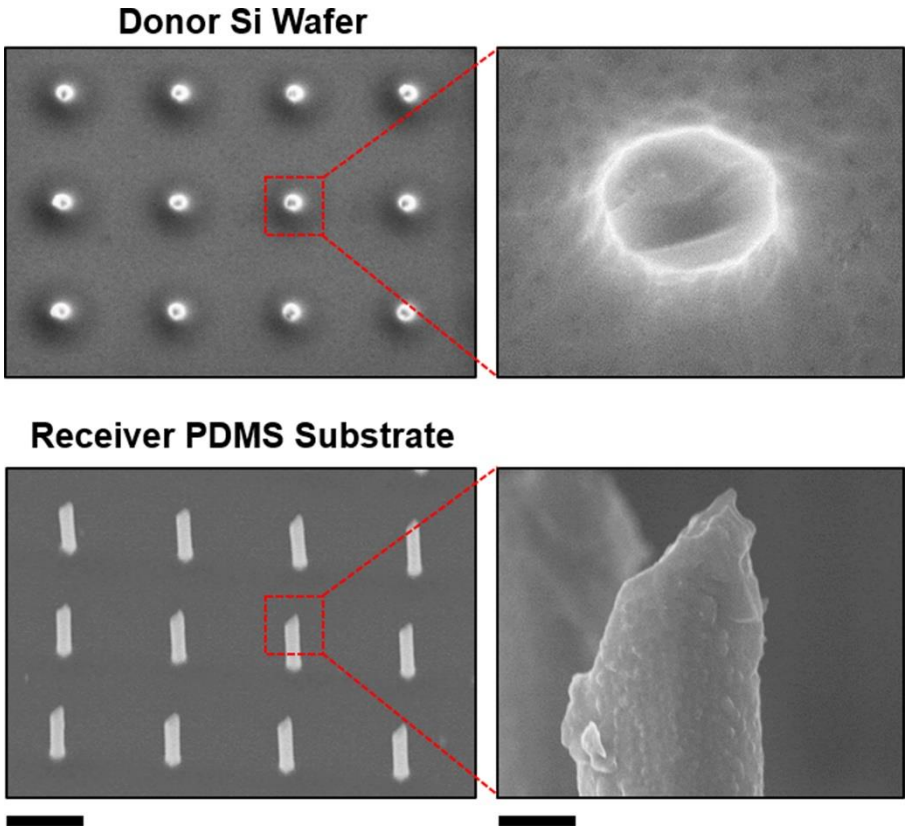

Fig. S1. SEM images (scale bar, 10 μm) of the donor Si wafer and the receiver PDMS substrate after the physical separation process, with their enlarged images (scale bar, 1 μm).

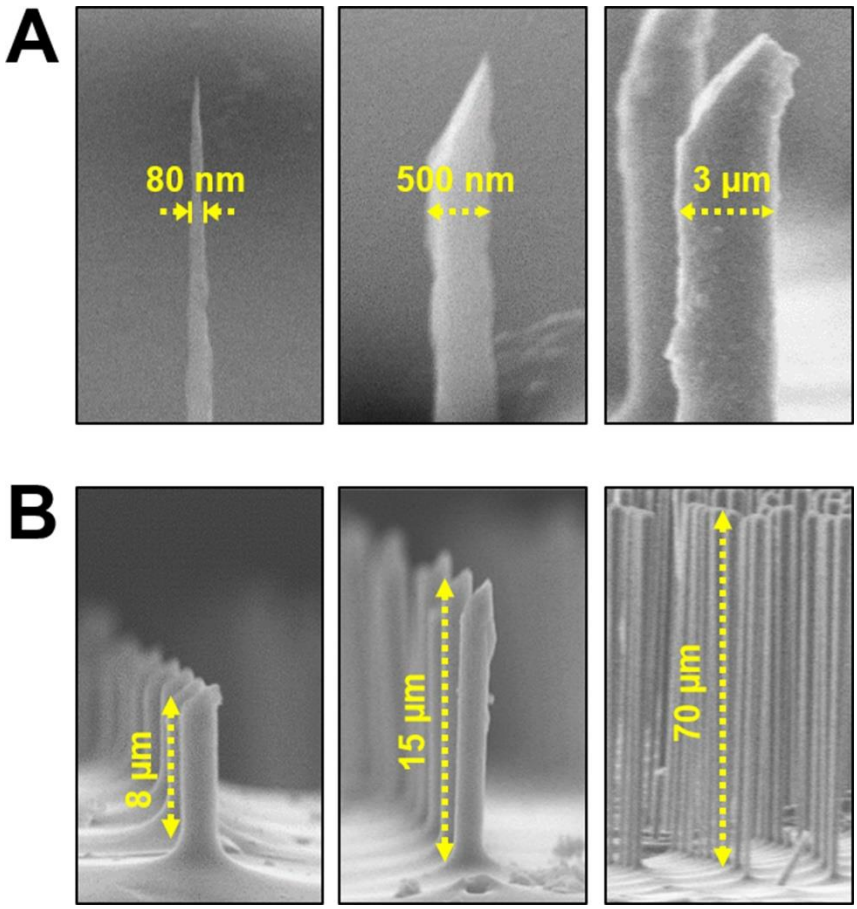

Fig. S2. SEM images of Si NNs with varied tip size (**A**) and height (**B**).

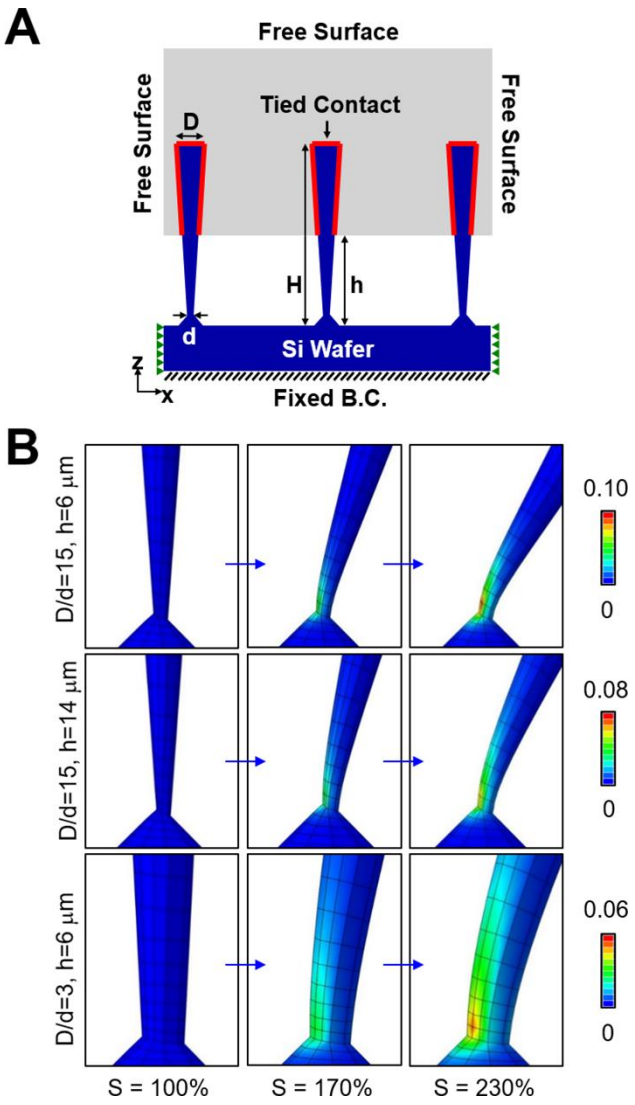

Fig. S3. (**A**) Schematic illustration for modeling geometry and boundary conditions and (**B**) computational results (FEA) of strain distributions of a single Si NN under deformations at varied *D/d* ratio, *h*, and *S*.

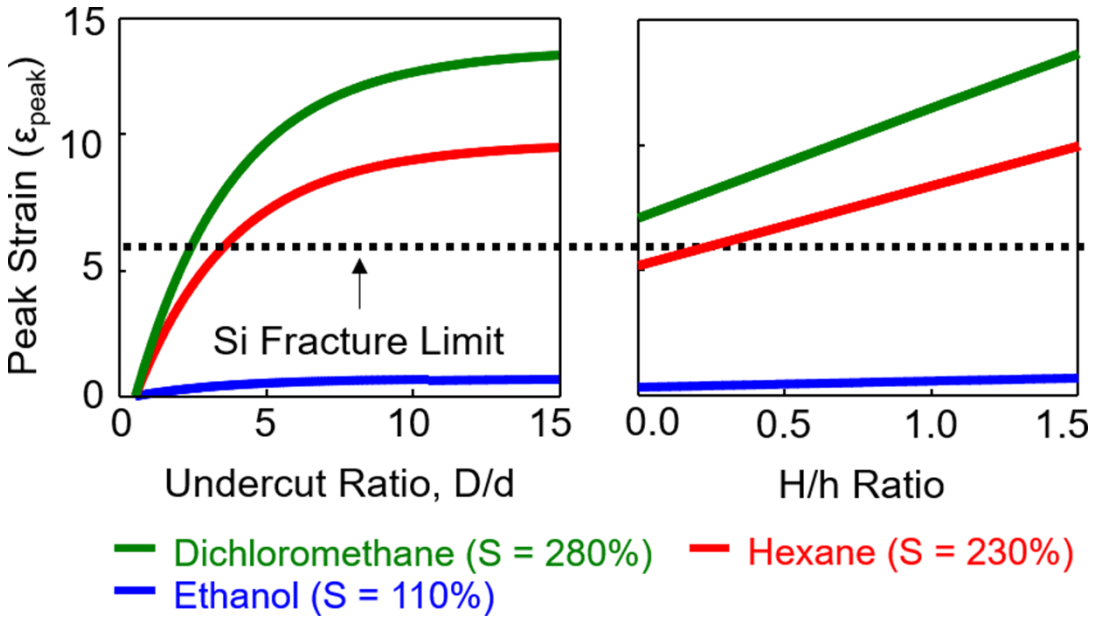

Fig. S4. Computational (FEA) data showing the effect of peak strain (ε_{peak}) on *D*/*d* ratio and *H*/*h* ratio using dichloromethane (green), hexane (red), and ethanol (blue). Black dotted line denotes the theoretical fracture limit of the Si NN.

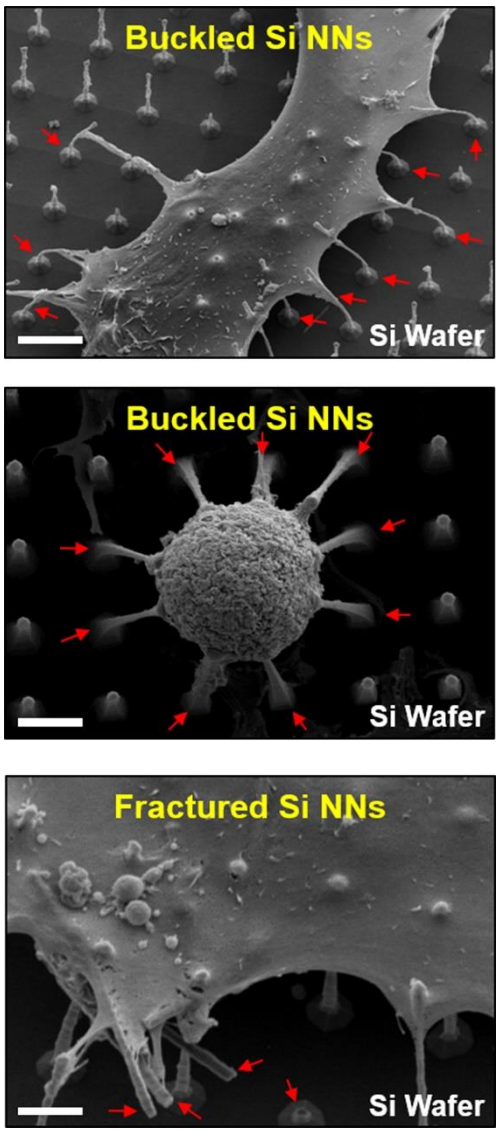

Fig. S5. SEM images (scale bars, 7, 5, and 3 μm from the top) of cells interfaced with control Si NNs built on a bulk Si wafer.

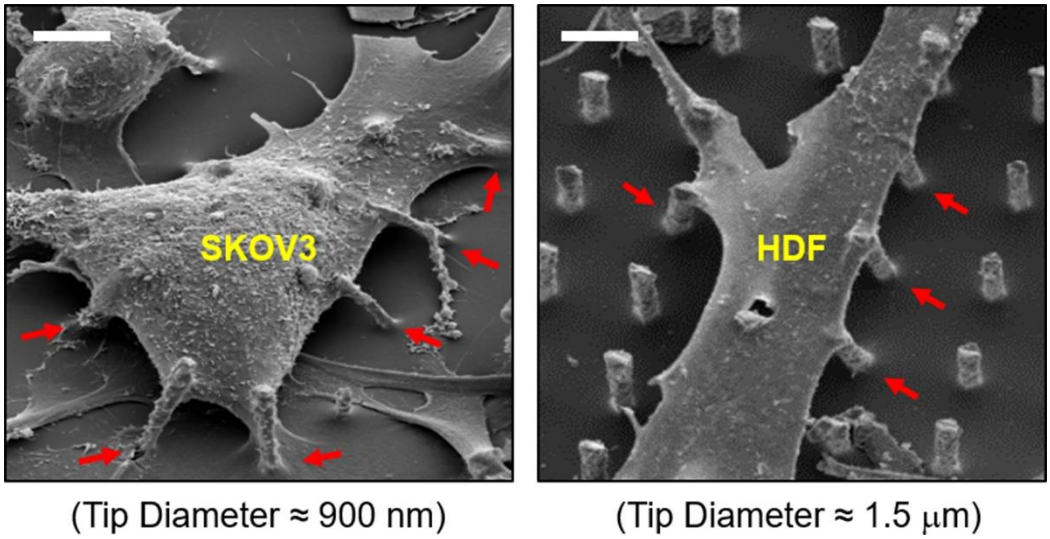

Fig. S6. SEM images (scale bars, 7 and 10 μm from the left) of SKOV3 cells (left) and HDF cells (right) interfaced with different sizes of Si NNs at the bottom.

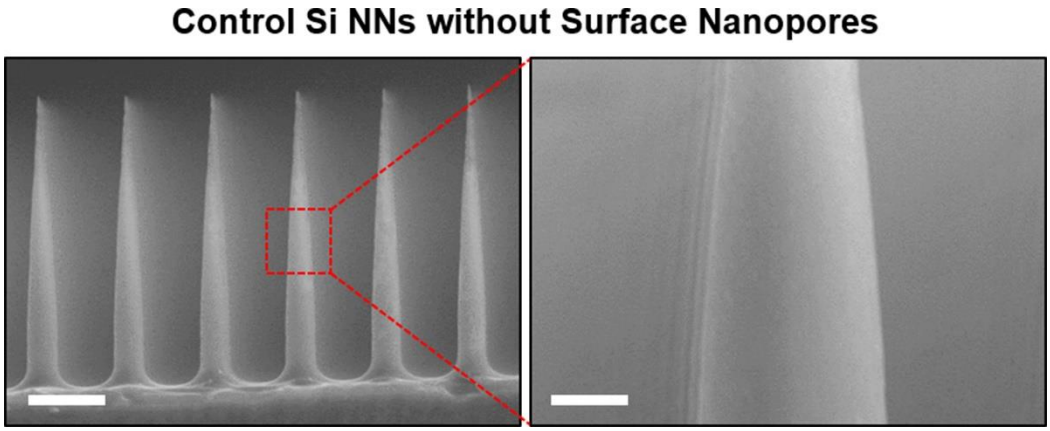

Fig. S7. SEM images (scale bars, 5 and 1.5 μm from the left) of control Si NNs without the nanoscale pores on the surface.

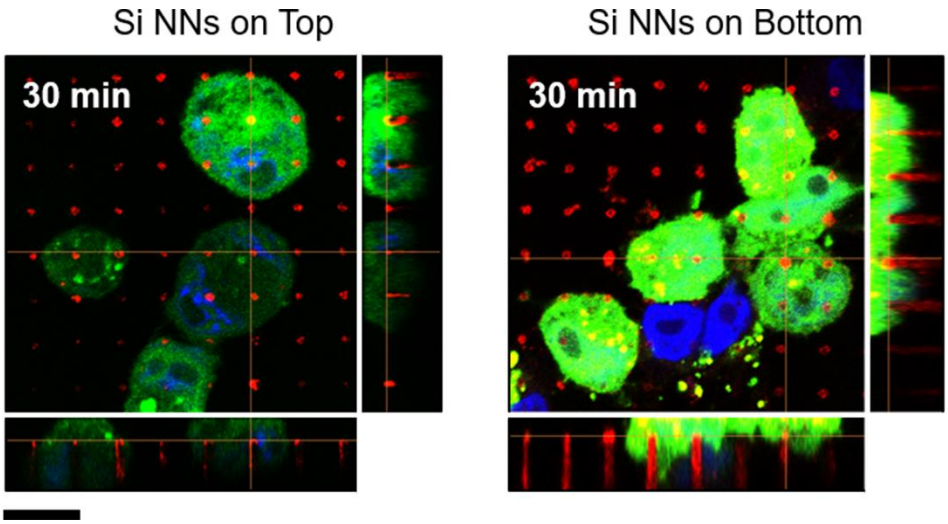

Fig. S8. Confocal microscopy images (scale bar, 10 μm) of the cultured MCF7 cells at 30 min after nanoinjection by either pressing Si NNs on top (left) or seeding the cells on Si NNs (right).

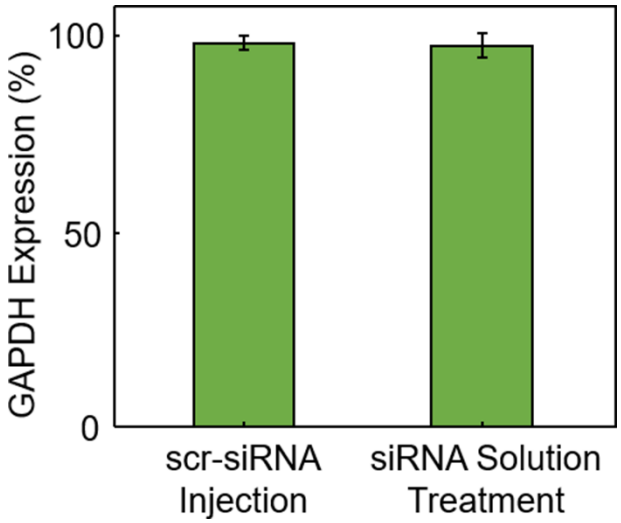

Fig. S9. Measured GAPDH expression by a control nanoinjection of scrambled siRNAs (left) and a control treatment in the siRNA solution (right).

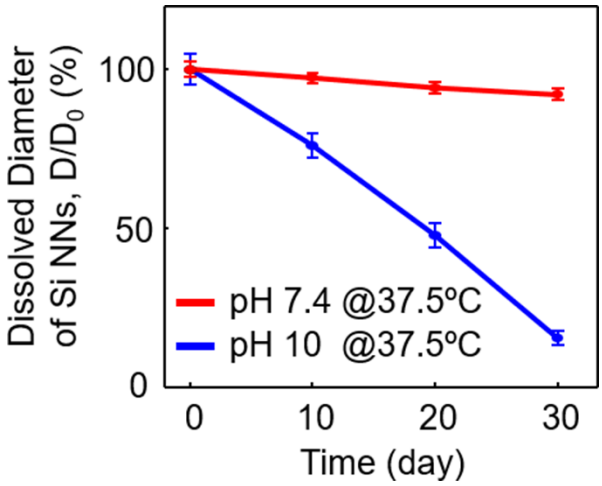

Fig. S10. Dissolved diameter (D/D0 ratio) of nanoporous Si NNs in a PBS solution with pH values of 7.4 (red) and 10 (blue) at 37.5°C.

Captions for Movies

Movie S1. An experimental demonstration (scale bar, 2.5 mm; 20× speed) showing the expansion of PDMS when soaked in hexane.

Movie S2. FEA results of displacement for a simplified structure that includes an array (3 cm × 3 cm) of Si NNs on a thin layer of PDMS under the expansion up to 230% in volume.

Movie S3. Continuously recorded live DIC image (scale bar, 15 μm; 4000× speed) of MCF7 cells for 36 hours.

Movie S4. A continuously recorded movie (scale bar, 2 cm; 1× speed) showing a mouse awake with the attached Si NN-patch on the skin.

Movie S5. A continuously recorded movie (scale bar, 2 cm; 1× speed) showing a mouse awake with the implanted Si NN-patch on the subcutaneous muscle.